Signal Design for Ultra-Wideband Radar and Wireless Communications

MALEK G. M. HUSSAIN
Electrical Engineering Department
Kuwait University
P. O. Box 5969; Al-Safat 13060
KUWAIT

Abstract: - The emerging ultra-wideband technology is in demand of extensive theoretical as well as experimental research to advance the implementation and commercial use of its numerous applications. Impulse-type signals are characterized by an ultra-wide frequency bandwidth that is desirable for the applications of high-resolution radar and wireless communications. In this paper, a signal model referred to as the generalized Gaussian pulse is derived for the analytical representation of electromagnetic impulses used in the experimentation of ultra-wideband technology. The signal characteristics of the generalized Gaussian pulse are analyzed. Computer plots of the time variation, autocorrelation function, and energy spectral density are also presented. The structure of a spread-spectrum signal for the ultra-wideband impulse technology is described too.

Key-Words:-Ultra-widband signals, impulse waveforms, impulse radar, signal design

1 Introduction

The rapid technological advances in microwave-energy sources and the solid-state electronic and opto-electronic switching devices have made it possible to generate and radiate high energy ultra-wideband (UWB) electromagnetic (impulse-type) signals. The combined low-frequency components and ultra-wide frequency bandwidth is an attractive feature of UWB impuls-type signals. Such signals have found numerous applications for radar and wireless communications, where significant advantages in performance, cost, and component size can be achieved over that offered by the conventional (narrowband) systems [1]–[3].

The design and modeling of impulse-type signals are essential for the development of the principles and applications of UWB impulse technology. In practice, impulse-type signals should satisfy a set of essential criteria: (i) the time-function, or model, of the signal is causal so that a physically-realizable radiator and a "matched filter" (or correlator receiver) can be implemented; (ii) the signal model has attractive autocorrelation properties, like a spike with no time-sidelobes, to yield a high resolution capability; (iii) the energy spectral density of the signal is free from a dc-component to allow for its efficient radiation by an impulse antenna; (iv) the time function of the signal is (mathematically) simple for developing the signal processing theory for the UWB impulse technology.

In Section II, we first describe the structure of spread-spectrum (SS) signals for the applications of impulse communications and impulse radar. We also derive a realistic signal model for the analytical representation of electromagnetic impulses generated in the experimentation of UWB impulse technology. The signal model is referred to as the generalized Gaussian pulse (GGP). In Section III, the autocorrelation function and the energy spectral density of the GGP model are presented and plotted to show that they satisfy the above design criteria. Conclusions are given in Section IV.

2 Signal Models for Impulse Technology

The characteristics of different impulse-type waveforms are described. The waveforms are useful for developing the theory and analysis of impulse radar and radio communications.

2.1 Spread Spectrum Signals

In the applications of impulse technology, the structure of a transmitted signal $x(t)$ is composed of a train of N UWB impulses analytically expressed as

follows [4]–[6],

$$x(t) = \sum_{n=0}^{N-1} q_n \Omega\left(t - nT_r - c_n T_c - T_d D_i\right). \quad (1)$$

In (1), T_r is the pulse repetition interval (PRI), $\Omega(t)$ is the shaping signal, $\{q_n\}$ is a binary psuedo-random (PN) code of length N and elements +1 or -1, $\{c_n\}$ is also a PN code referred to as the time-hopping (TH) code with integer elements in the range $0 \leq c_n \leq N_h$, $T_c \ll T_r$ is the chip duration of the TH code, and $T_d \ll T_r$ is the data-modulation time shift that conveys to the receiver information regarding the symbol $D_i = i, i = \{0, 1\}$. The symbol duration is $T_s = NT_r$, and the binary symbol rate is $R_s = 1/T_s = 1/NT_r$. The maximum time-hopping interval is $N_h T_c \leq T_r$. In this case, information transmission is accomplished via *pulse-position modulation* (PPM) while multiple-access capability is achieved by the PN code q_n or the TH code c_n depending on the type of the spread-spectrum-modulaion technique being used.

For example, digital-impulse-radio communication systems transmit binary data symbols (0 and 1) by coded sequences of N UWB impulses. The coding scheme can either be applied to the PRI, or directly to the amplitude of the individual pulses depending on the system complexity. The coding (or staggering) of the PRI is referred to as *time-hopping* (TH) SS modulation [5]. The amplitude coding scheme is the same as the well known *direct-sequence* (DS) SS modulation. Also, it is possible to implement a *hybrid* DS-TH coding scheme which yields improved system capacity and security, but on the account of a more costly and complex system. The hybrid DS-TH modulation scheme is analogous to the known hybrid direct-sequence and frequency-hopping (DS-FH) spread spectrum technique. The SS signal model in (1) represents a general DS-TH-SS signal that is well suited for the applications of impulse technology.

The signal structure given in (1), with $T_d = 0$, can also represent a radar signal having a low probability of intercept, and high resistance against jamming [4]. This "stealthy" feature of impulse-type signals is one of the potential advantages of UWB impulse technology [1]–[3].

The energy spectral density of the shaping signal $\Omega(t)$ in (1) must be free from a direct-current (dc) component, since according to antenna principles, the presence of a dc component in the spectrum of a baseband pulse prevents the radiation of its electromagnetic field intensity without an appropriate form of signal modulation using a sinusoidal carrier. The focus of this paper is on the analytical design of a suitable shaping signal $\Omega(t)$ for the carrier-free applications of UWB impulse technology.

2.2 Monocycle Gaussian Pulse and Richard Wavelet

In our experimentation with impulse technology, an intricate UWB antenna system generates, at a very high rate, the current pulse shown in Fig. 1(a) and radiates the signal shown in Fig. 1(b). In principle, the time variation of the radiated signal in Fig. 1(b) is directly proportional to the first derivative of the antenna current in Fig. 1(a) [2]. Based on this fundamental relationship, we shall derive theoretical (signal) models for the measured antenna current and the radiated impulse-type signal in Fig. 1. The signal models are essential for developing the signal processing theory of impulse technology.

Consider the well known Gaussian distribution function, referred to here as Gaussian pulse $g(t)$, and its Fourier transform $G(f)$,

$$g(t) = E_\circ \exp\{-\pi[(t - t_\circ)/\Delta T]^2\}, \quad (2)$$

$$G(f) = \frac{E_\circ}{\Delta f} \exp\{-j2\pi f t_\circ\} \exp\{-\pi[f/\Delta f]^2\} \quad (3)$$

where $E_\circ$ is the peak amplitude at the time instance $t = t_\circ$, ΔT the effective duration, and $\Delta f = 1/\Delta T$ the effective frequency bandwidth.

The Gaussian pulse $g(t)$ given in (2) is very convenient mathematically as well as from the practical point of view for the design and theoretical modeling of the impulse-type signals shown in Fig. 1. According to (3), the frequency spectral density $G(f)$ includes a dc-component at $f = 0$; $|G(0)| \neq 0$. Consequently, an ideal Gaussian pulse $g(t)$ cannot be emitted by an impulse radiator due to the presence of the dc-component $|G(0)| = E_\circ/\Delta f$. On the other hand, the frequency spectrum of the first-order time-derivative $dg(t)/dt$ and that of the second-order time-derivative $d^2g(t)/dt^2$ of the Gaussian pulse $g(t)$ given in (2) include no dc component. The derivative $dg(t)/dt$ is referred to as the *monocycle Gaussian pulse*,

$$\frac{dg(t)}{dt} = -E_\circ[2\pi(t - t_\circ)/\Delta T^2] \exp\{-\pi[(t - t_\circ)/\Delta T]^2\}. \quad (4)$$

The second derivative $d^2g(t)/dt^2$ is the *Richard wavelet*,

$$\frac{d^2g(t)}{dt^2} = E_\circ\left[(2\pi(t - t_\circ))^2/\Delta T^4 - 2\pi/\Delta T^2\right] \times \exp\{-\pi[(t - t_\circ)/\Delta T]^2\}. \quad (5)$$

If one obtains a plot for the monocycle Gaussian pulse given in (4), it will look similar in shape to the transient current shown in Fig. 1(a). A plot for the Richard wavelet given in (5) will look identical to the impulse signal shown in Fig. 1(b). Hence, the signal models in (4) and (5) are good analytical representations of the experimental signals shown in Fig. 1. But, the disadvantage of these two signal models is

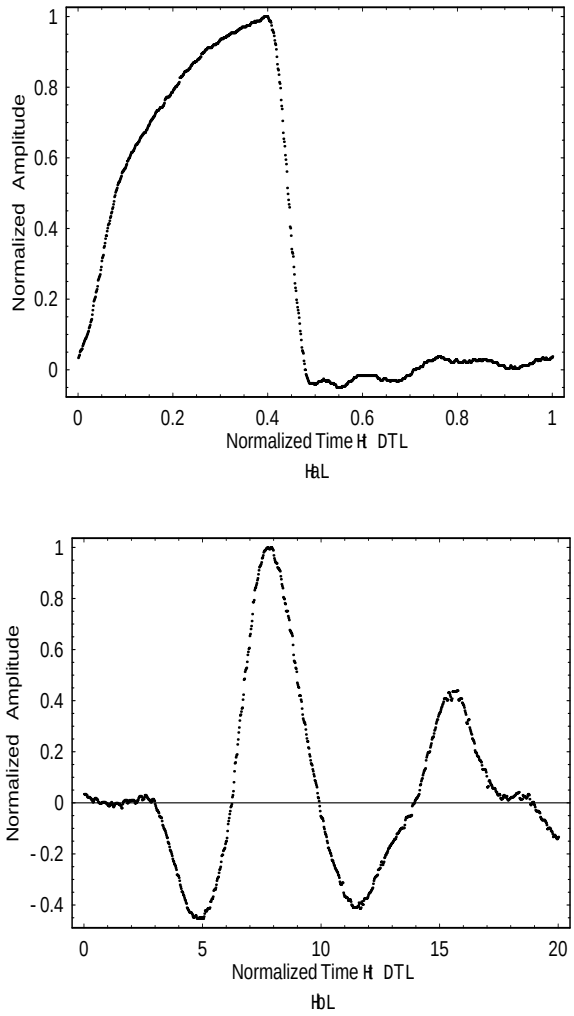

Fig. 1. Time variation of a voltage transient that is directly proportional to a current pulse, $i(t)$, generated for driving an UWB antenna (a), and the radiated electromagnetic impulse, $e(t) = -di(t)/dt$,(b).

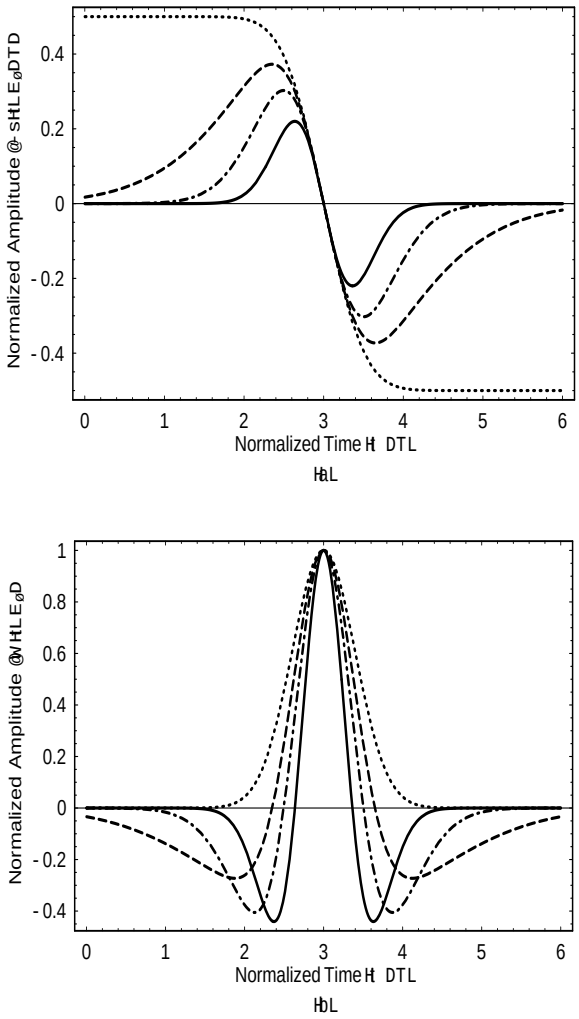

Fig. 2. The normalized time variation of $-s(t)/E_\circ \Delta T$ (a), and that of the generalized Gaussian pulse $\Omega(t) = ds(t)/dt$ (b), as functions of relative time $t/\Delta T$, for $t_\circ/\Delta T = 3$, and the values of the scale parameter $\alpha = 0$ (dotted-line), $\alpha = 0.3$ (dashed-line), $\alpha = 0.6$ (dashed-dotted-line), and $\alpha = 1.2$ (solid-line).

that they are not mathematically simple for developing the advanced signal processing theory for UWB impulse technology. The product of the term $(t - t_\circ)$ with the exponential function in (4) and (5) makes the two functions intricate to work with. Simpler signal models are derived in the following section.

2.3 Generalized Gaussian Pulse

Let the Gaussian pulse $g(t)$ given in (2) be scaled in time duration by the *scale parameter* α to obtain,

$$g(\alpha t) = E_\circ \exp\{-\pi[\alpha(t - t_\circ)/\Delta T]^2\}. \qquad (6)$$

The difference between the integral of the Gaussian pulse $g(t)$ and that of the pulse $g(\alpha t)$ yields a time function, $s(t)$, that is a suitable analytical representation for the experimental antenna current shown in Fig. 1(a). This time function is expressed as follows,

$$\begin{aligned} s(t) &= \frac{1}{1-\alpha}\left(\int_0^t g(t')\,dt' - \int_0^t g_(\alpha t')\,dt'\right) \\ &= \frac{E_\circ \Delta T}{\sqrt{\pi}(1-\alpha)}\left(\int_0^{\sqrt{\pi}(t-t_\circ)/\Delta T} \exp\{-u^2\}\,du \right. \\ &- \left. \int_0^{\sqrt{\pi}\alpha(t-t_\circ)/\Delta T} \exp\{-u^2\}\,du\right). \qquad (7) \end{aligned}$$

Each one of the two integrals in (7) has the form of the well known *error function*: $\mathrm{erf}(t) = (2/\sqrt{\pi})\int_0^t e^{-u^2}\,du$. Hence, the two integrals in (7) result in the signal

$$\begin{aligned} s(t) &= \frac{E_\circ \Delta T}{2(1-\alpha)} \\ &\times \mathrm{Erf}\left[\{\sqrt{\pi}\alpha(t-t_\circ)/\Delta T\}\,,\right. \\ &\left.\{\sqrt{\pi}(t-t_\circ)/\Delta T\}\right], \qquad (8) \end{aligned}$$

where the function $\mathrm{Erf}[t_1, t_2]$ is the *generalized error*

function,

$$\text{Erf}[t_1, t_2] = \frac{2}{\sqrt{\pi}} \int_{t_1}^{t_2} \exp\{-u^2\}\, du = \text{erf}[t_2] - \text{erf}[t_1]. \tag{9}$$

The derivative $ds(t)/dt$ results in the signal

$$\begin{aligned} \Omega(t) &= \frac{ds(t)}{dt} \\ &= \frac{E_\circ}{1-\alpha} \left(\exp\{-\pi[(t-t_\circ)/\Delta T]^2\}\right. \\ &- \left. \alpha \exp\{-\pi[\alpha(t-t_\circ)/\Delta T]^2\}\right), \alpha \neq 1. \end{aligned} \tag{10}$$

The factors α and $1/(1-\alpha)$ in (10) suppress the dc-component from the frequency spectrum of the signal $\Omega(t)$; the energy density spectrum of $\Omega(t)$ will be presented in Section III.

The function $\Omega(t)$ is referred to as the *generalized Gaussian pulse* (GGP). Computer plots of the normalized signals $-s(t)/E_\circ \Delta T$ given in (8) and $\Omega(t)/E_\circ$ given in (10) are shown in Fig. 2 (a) and (b), respectively. The signals are plotted as functions of the relative time $t/\Delta T$, for $t_\circ/\Delta T = 3$, and different values of the scale parameter $\alpha = 0$, 0.3, 0.6, and 1.2.

According to Fig. 2, as the value of α is increased the GGP waveform becomes more compressed in time, which results in spreading of its frequency spectrum. For $\alpha = 0$, the time variation of the GGP $\Omega(t)$ reduces to that of the ideal Gaussian pulse $g(t)$ given in (2). Therefore we used the name generalized Gaussian pulse for $\Omega(t)$. A comparison between the experimental impulse-type signal in Fig. 1(b) and the theoretical signal $\Omega(t)$ in Fig. 2(b) shows that the two signals are identical in shape for $\alpha > 0$; the secondary positive lobe in Fig. 1(b) is an echo. The same comparison holds for the measured transient in Fig. 1(a) and the theoretical signal $-s(t)$ shown in Fig. 2(a). Hence, for $\alpha > 0$ the signal model $s(t)$ given in (9) and the GGP model, $\Omega(t)$ given in (10) are appropriate analytical representations for the experimental signals in Fig. 1(a) and (b), respectively.

The time function $\Omega(t)$ given in (10) is purely an exponential function of relative time $(t/\Delta T)$. This is a much simpler function, from mathematical and signal analysis points of view, than the function $d^2g(t)/dt^2$ defined in (5).

3 Autocorrelation Function and Energy Density Spectrum

The autocorrelation function and the energy density spectrum of a signal play an important role in the design and the performance evaluation of radar and radio communication systems. For the GGP signal $\Omega(t)$, the auocorrelation function $\Upsilon(t) = \int_{-\infty}^{\infty} \Omega(\lambda)\Omega(\lambda + t)\, dt$ yields, for the time $t_\circ = 0$,

$$\begin{aligned} \Upsilon(t) &= \left(\frac{E_\circ}{1-\alpha}\right)^2 \frac{\Delta T}{\sqrt{2}} \\ &\times \left(\exp\{-[\pi/2][t/\Delta T]^2\}\right. \\ &+ \alpha \exp\{-[\pi\alpha^2/2][t/\Delta T]^2\} \\ &- [8\alpha^2/(1+\alpha^2)]^{1/2} \\ &\times \left. \exp\{-[\pi\alpha^2/(1+\alpha^2)][t/\Delta T]^2\}\right). \end{aligned} \tag{11}$$

The normalized autocorrelation function $\Upsilon(t)/\Upsilon(0)$ is plotted in Fig. 3(a), as a function of relative time $t/\Delta T$, for different values of the scale parameter $\alpha =$ 0, 0.3, 0.6, and 1.2. The energy $\mathcal{E}$ of the GGP signal $\Omega(t)$ can be determined from the peak value of its autocorrelation function at $t = 0$,

$$\mathcal{E} = \Upsilon(0) = \frac{E_\circ^2 \Delta T}{\sqrt{2}(1-\alpha^2)} \left[1 + \alpha - \left(\frac{8\alpha^2}{1+\alpha^2}\right)^{1/2}\right]. \tag{12}$$

According to Fig. 3(a), the autocorrelation function $\Upsilon(t)$ is comprised of a distinguishable mainlobe centered at $t/\Delta T = 0$, and time-sidelobes with positive as well as negative amplitudes distributed along each side of the mainlobe. The duration of the mainlobe becomes narrow and the levels of the time-sidelobes increase for the increasing values of the scale parameter α. For $\alpha = 0$, $\Upsilon(t)$ has a Gaussain time variaton with no sidelobes; this case corresponds to the autocorrelation function of the ideal Guassian pulse $g(t)$ given in (2) with $t_\circ = 0$.

The energy density spectrum $\Psi(f)$ of the GGP signal $\Omega(t)$ is determined by the Fourier transform of its autocorrealtion function $\Upsilon(t)$,

$$\Psi(f) = \int_{-\infty}^{\infty} \Upsilon(t) \exp\{-j2\pi f t\}\, dt. \tag{13}$$

Insertion of (11) into (13) results in the energy density spectrum

$$\begin{aligned} \Psi(f) &= \left[\frac{E_\circ}{(1-\alpha)\Delta f}\right]^2 \left(\exp\{-2\pi[f/\Delta f]^2\}\right. \\ &+ \exp\{-[2\pi/\alpha^2][f/\Delta f]^2\} \\ &- \left. 2\exp\{-[\pi(1+\alpha^2)/\alpha^2][f/\Delta f]^2\}\right). \end{aligned} \tag{14}$$

The energy density spectrum $\Psi(f)/(E_\circ/\Delta f)^2$ is shown in Fig. 3(b), as a function of the relative frequency $f/\Delta f$, for different values of the scale parameter $\alpha =$ 0, 0.3, 0.6, and 1.2. For $\alpha > 0$, the energy density specrum $\Psi(f)$ does not include a dc-component at $f/\Delta f = 0$; $\Psi(0) = 0$. Hence, the GGP signal $\Omega(t)$ given in (10), the signal $s(t)$ given in (8), the autocorrelation function $\Upsilon(t)$ given in (11), and the energy density spectrum $\Psi(f)$ given in (14), satisfy all the signal characteristics required for the operation of UWB impulse technology. According to Fig. 3(b), the peak amplitude of the energy density spectrum $\Psi(f)$ decreases and shifts to a higher *center frequency* as the value of α is increased. This feature is a useful modulation tool for the design of UWB impulse type waveforms used in the applications of radar and aradio communications.

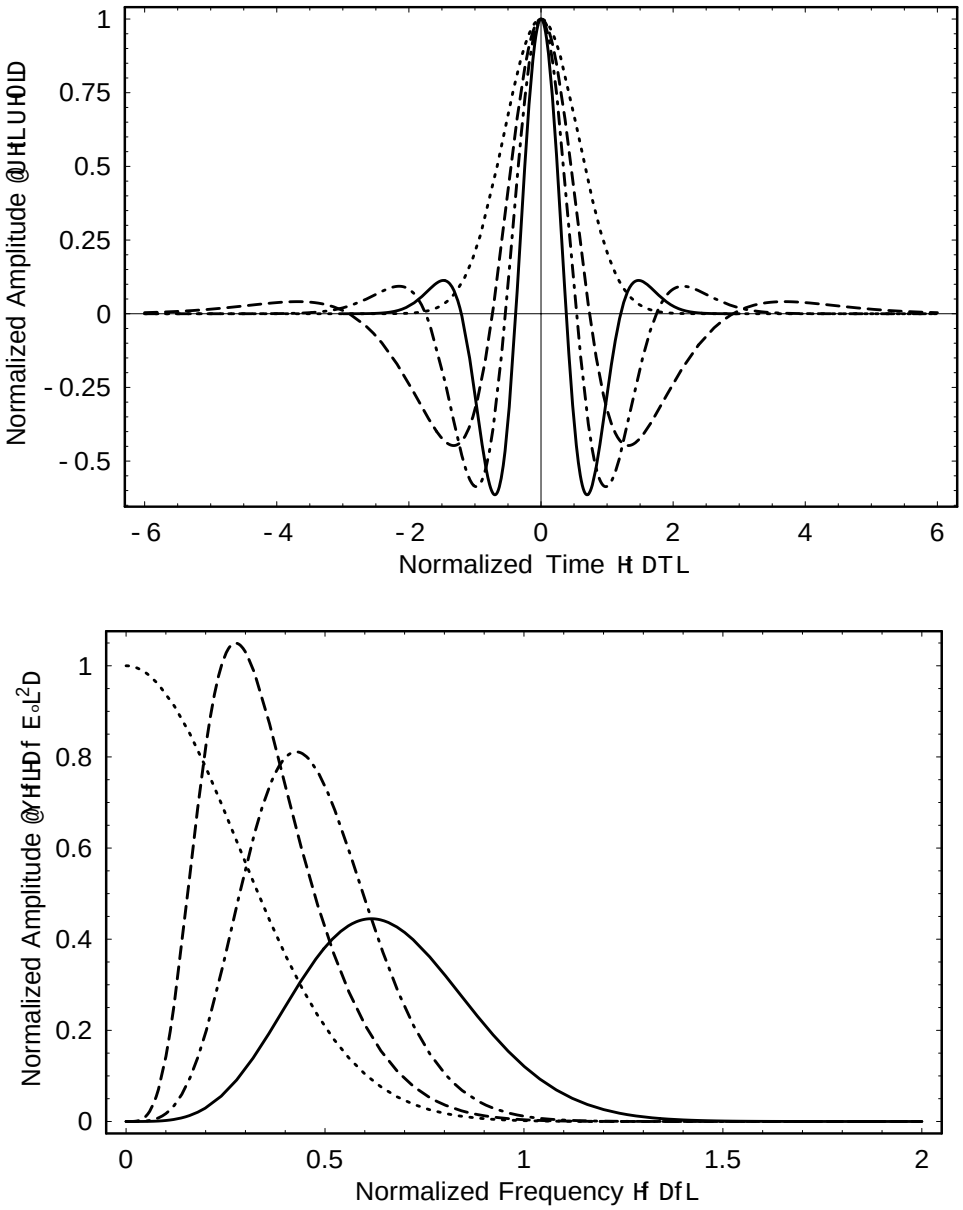

Fig. 3. The normalized autocorrelation function $\Upsilon(t)/\Upsilon(0)$ (a), and the normalized energy spectral density $\Psi(f)[\Delta f/E_\circ]^2$ (b), plotted for the values of the scale parameter $\alpha = 0$ (dotted-line), $\alpha = 0.3$ (dashed-line), $\alpha = 0.6$ (dashed-dotted-line), and $\alpha = 1.2$ (solid-line).

4 Conclusions

An analytical signal model is derived for the representation of UWB electromagnetic impulses generated for the applications of radar and wireless communications. The signal model is referred to as the generalized Gaussian pulse, GGP. The signal characteristics of the GGP model are attractive for the development of the signal processing theory for the emerging UWB impulse technology.

References:

[1] Taylor,J. D., ed., *Introduction to Ultra-wideband radar Systems.* CRC Press, Florida, 1995.

[2] Hussain, M. G. M., "Ultra-wideband impulse radar-An overview of pinciples," *IEEE AES Magazine,* vol. 13, no. 9, pp. 9-14, Sept. 1998.

[3] Harmuth, H. F., R. N. Boules, and M.G. Hussain. *Electromagnetic Signals:Reflection, Focusing, Distortion, and Their Practical Applications.* Kluwer Academic/Plenum, New York, 1999.

[4] Hussain, M. G. M., "Principles of high-resolution radar based on nonsinusoidal waves-Part I: Signal representation and pulse compression," *IEEE Trans.Electromagn. Compat.,* vol. EMC-31, no. 4, pp. 359-368, Nov. 1989.

[5] Scholtz, R. A., Multiple access with time-hopping impulse modulation," *Proc. IEEE MILCOM'93,* Boston, MA, Oct. 11–14, 1993.

[6] Win, M. Z., and Scholtz, R. A., Impulse Radio: How it works," *IEEE Comm. Letters,* vol. 2, no. 2, pp. 36–38, Feb. 1998.